

2004

Stratigraphic Continuity in 400 Mhz Short-Pulse Radar Profiles of Firn in West Antarctica

Steven A. Arcone

Vandy Blue Spikes

Gordon S. Hamilton

University of Maine - Main, gordon.hamilton@maine.edu

Paul Andrew Mayewski

University of Maine - Main, paul.mayewski@maine.edu

Follow this and additional works at: https://digitalcommons.library.umaine.edu/ers_facpub



Part of the [Earth Sciences Commons](#)

Repository Citation

Arcone, Steven A.; Spikes, Vandy Blue; Hamilton, Gordon S.; and Mayewski, Paul Andrew, "Stratigraphic Continuity in 400 Mhz Short-Pulse Radar Profiles of Firn in West Antarctica" (2004). *Earth Science Faculty Scholarship*. 143.

https://digitalcommons.library.umaine.edu/ers_facpub/143

This Conference Proceeding is brought to you for free and open access by DigitalCommons@UMaine. It has been accepted for inclusion in Earth Science Faculty Scholarship by an authorized administrator of DigitalCommons@UMaine. For more information, please contact um.library.technical.services@maine.edu.

Stratigraphic continuity in 400 MHz short-pulse radar profiles of firn in West Antarctica

Steven A. ARCONE,¹ Vandy B. SPIKES,² Gordon S. HAMILTON,² Paul A. MAYEWSKI²

¹US Army Engineer Research and Development Center, Cold Regions Research and Engineering Laboratory, Hanover, NH 03755, USA

E-mail: Steven.A.Arcone@erdc.usace.army.mil

²Climate Change Institute, University of Maine, 303 Bryand Global Sciences Center, Orono, ME 04469, USA

ABSTRACT. We track dated firn horizons within 400 MHz short-pulse radar profiles to find the continuous extent over which they can be used as historical benchmarks to study past accumulation rates in West Antarctica. The 30–40 cm pulse resolution compares with the accumulation rates of most areas. We tracked a particular set that varied from 30 to 90 m in depth over a distance of 600 km. The main limitations to continuity are fading at depth, pinching associated with accumulation rate differences within hills and valleys, and artificial fading caused by stacking along dips. The latter two may be overcome through multi-kilometer distances by matching the relative amplitude and spacing of several close horizons, along with their pulse forms and phases. Modeling of reflections from thin layers suggests that the –37 to –50 dB range of reflectivity and the pulse waveforms we observed are caused by the numerous thin ice layers observed in core stratigraphy. Constructive interference between reflections from these close, high-density layers can explain the maintenance of reflective strength throughout the depth of the firn despite the effects of compaction. The continuity suggests that these layers formed throughout West Antarctica and possibly into East Antarctica as well.

INTRODUCTION

Long-distance radar horizons in polar firn used to study past snow-accumulation rates require accurate benchmark horizons that can be tracked, if possible, for hundreds to thousands of kilometers. Although the synthetic pulse radars used to record these horizons operated at bandwidths centered as high as 750 (Kanagaratnam and others, 2001) and 1500 MHz (Richardson and others, 1997), they detect envelopes of modulation, so the horizons last several cycles of the center bandwidth frequency and appear unstructured. Therefore, they may have masked closely spaced reflections at the decimeter or annual scale. This lack of resolution can be disadvantageous where increased wind speed in hilly areas reduces accumulation rates (Van der Veen and others, 1999) and over long distances such as in West Antarctica, where snow-accumulation rates can vary from 35 to possibly 200 cm a⁻¹ in the eastern part. Closely aligned with the continuity problem is the nature of the horizons. Although it is well established that firn horizons are related to density contrasts (e.g. Fujita and others, 1999; Eisen and others, 2003), complex pit and trench stratigraphy (Benson, 1971) makes it unclear what type of density anomaly might persist for hundreds of kilometers at decimeter resolution. In this paper, we examine horizon continuity at a radar pulse resolution of about 35 cm and speculate on its cause.

Our objectives are to find the spatial extent of horizons composed of single high-resolution pulses, the factors that limit or interrupt their continuity, the structure of the pulses, and the range of their reflectivity values. We used a traditional, 300–500 MHz short-pulse radar (Arcone, 2002). We tracked horizons over hundreds of kilometers throughout central West Antarctica to depths near 90 m. We used pulse form and compared horizon sequences to establish continuity beyond relatively intense stratigraphic deformation, and we used core stratigraphy, horizon reflectivity, and modeling to investigate a possible cause

for the horizons. Our profiles were collected as part of the International Trans-Antarctic Scientific Expedition (ITASE; Mayewski, 2003) program to study recent Antarctic climate and mass balance.

Although our radar has a lower absolute bandwidth than the radars cited above, and far less penetration than the 750 MHz system, the 1½-cycle transmitted pulse provides an interface resolution of 30–40 cm in firn. The pulse waveform helps to identify the character of horizons and thus to track them across areas where continuity is lost. Theoretically the transmitted waveform or its inverse also changes insignificantly upon reflection from layers thinner than about 10 cm. We have used stratigraphic dating of core chemistry to establish the isochronal nature of these horizons to an accuracy of ±1 year (Spikes, 2003).

TRANSECTS

Radar data were collected along several traverse routes conducted from 1999 to 2002 (Fig. 1). The routes originate at Byrd Surface Camp (BSC). Transect I (1999) extends 181 km southwest from BSC and drops 560 m in elevation. The western half contains long, rolling hills of 30–60 m relief spaced on the order of 10 km, and it obliquely crosses the upper portion of Bindschadler Ice Stream (former Ice Stream D; Hamilton and Spikes, 2004). Much of transects II (2000) and III (2001) are in the vicinity of higher-accumulation zones near ice divides, and climb >300 m from BSC. Transect IV (2002) generally follows an ice divide to the South Pole, with relatively smooth topography for about the first 300 km.

EQUIPMENT, DATA PROCESSING AND WAVELET CHARACTERISTICS

We used a Geophysical Survey Systems Inc. model SIR 10B control unit and towed a 400 MHz model 5103 antenna

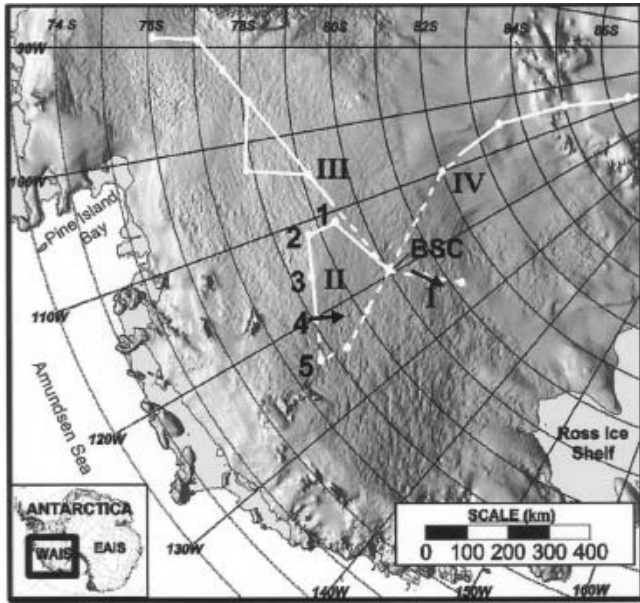


Fig. 1. ITASE transect and core site locations (dots). Year 2000 core sites are numbered. The visible extent of the particular horizons discussed in the text is indicated by the dotted lines radiating from BSC. Limited data were recorded from BSC to site 1.

transducer unit that rested on the bottom of a small sled. The sled maintained good surface contact because severe sastrugi were never encountered. The 4 ns (Fig. 2) pulse duration gives an interface resolution of about 35 cm in firn of refractive index $n = 1.5$ (density, $\rho = 600 \text{ kg m}^{-3}$). We used a running 32-fold stack to give an effective spatial recording rate of about 1 trace/2.7 m at an approximate traverse speed of 2 m s^{-1} for transect I, about 1 trace/15 m at the 3.3 m s^{-1} average speed of transects II and III, and about 1 trace/12 m at the 2.5 m s^{-1} speed of transect IV. We simultaneously recorded precise geodetic differential global positioning system (GPS) data to locate our position and elevation.

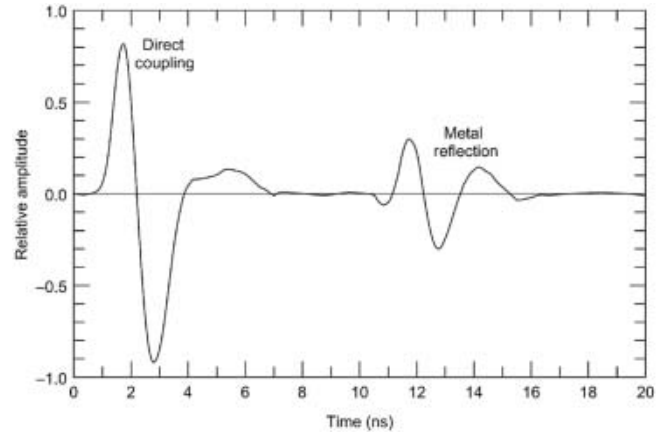


Fig. 2. The 400 MHz antenna waveforms. The amplitudes of the direct coupling between transmitter and receiver antennas and the metal reflection are cross-references used to measure reflectivity values for the firn horizons. The $+ - +$ phase polarity sequence (red-blue-red in the profiles) to the major half-cycles of the reflection is the inverse of that of the wavelet transmitted into the firn.

We adjusted our gain during processing to compensate only for the inverse dependency of amplitude upon range; two-way electric field transmission losses through firn interfaces are extremely insignificant. We removed constant-time-delay clutter from nearby equipment with a horizontal filter. The very small stratigraphic dips preclude the need for profile migration. We used the calibration between dielectric permittivity, ϵ , and snow density (Cumming, 1952) and the simple echo delay formula, $d = ct/2n$, to transform echo time delay, t , into depth, d , where $c = 0.3 \text{ m ns}^{-1}$ and $n = \sqrt{\epsilon}$. We applied the formula meter by meter from our core density profiles to obtain a variable depth scale. Common midpoint depth (CMP) gathers to verify velocities were not performed because cables are not available to accommodate the needed separations and

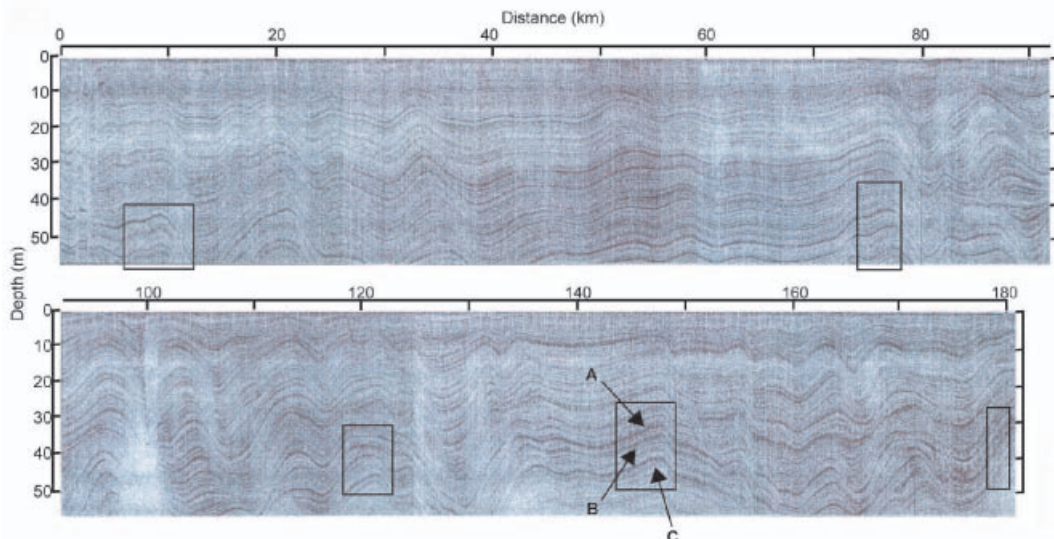


Fig. 3. Profile of transect I, from BSC going west. The boxes enclose the same set of three horizons, A–C, at least two of which were tracked along all transects in Figure 1. The depth scale is adjusted to the average relative dielectric permittivity, $\epsilon = 2.4$, for the depth of 56 m. The vertical exaggeration is 348:1. The stronger distortion occurs at 75–110 and 150–180 km, where the transect traversed a series of hills. Cores have been obtained at 0, 90 and 181 km.

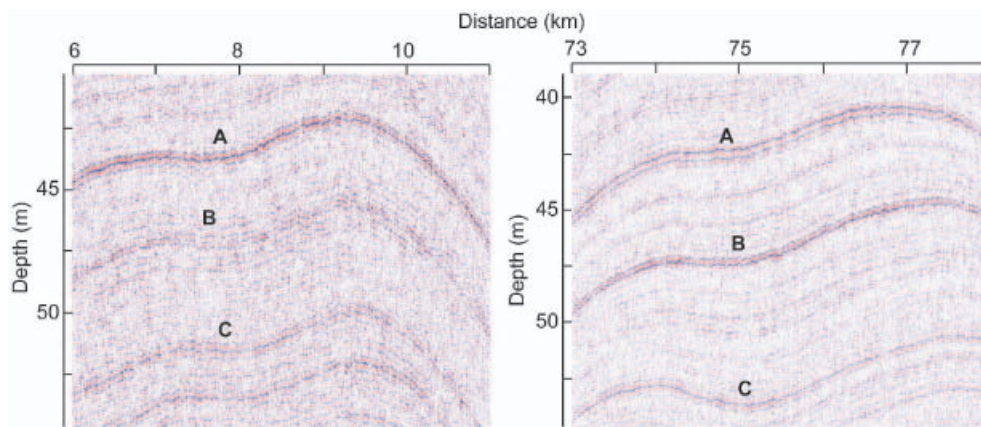


Fig. 4. Detail from Figure 3. Horizon A is composed of two closely spaced reflections that are separated enough (e.g. at 75 km) to show that they have opposite phase structures. The first of these and horizon C generally have a + + + phase sequence, while B has a - + - sequence.

because airwave references would not be recorded at such separations.

HORIZON CONTINUITY

We tracked three prominent horizons whose waveforms and relative separations allowed us to identify them along all four transects beyond areas where pinching and fading interrupted their continuity. The tie point along all transects for these horizons is at BSC. The three horizons are identified in transect I (Fig. 3), where they occur at depths of about 44.4, 47.4 and 51.9 m at BSC and at depths of 27, 30 and 32 m at the opposite end of transect I. They are dated to AD 1734, 1705 and 1666, respectively, by annual-layer counting (Kreutz and others, 2000; personal communication from S. Kaspari and D. Dixon, 2003). Horizon A often occurs as two closely spaced single wavelets, each with the opposite triad phase structure (Fig. 4). Horizons B and C also have the triad structure, the polarity sequence of which is consistent throughout the profiles. The folds occur where long, low hills are encountered, especially between 70 and 110 km, and are most likely caused by accumulation-rate variability (Van der Veen and others, 1999), primarily associated with leeward and windward slopes (Black and Budd, 1964). We think that some of the hinge axes do not migrate at all down-ice (east to west) with depth (e.g. near 113 and 175 km) because our transect was at about 20–25° to the flow, which could have kept us over synclinal hinges for several kilometers when crossing the hills, and because the variation of accumulation with slope (Black and Budd, 1964) may cause the apparent deformation and affect its migration. Real folding, caused by ice compression, does not seem possible because the velocity difference between BSC (11 m a⁻¹) and the end of transect I (48 m a⁻¹) implies extensional ice flow.

We can track one or two of these horizons along the other transects to the extent indicated by dashed lines in Figure 1. Horizon B extends south about 334 km along transect IV (Fig. 5) until deformation destroys the continuity for hundreds of kilometers. The forms of the pulses highlighted in Figure 5 do not occur consistently from trace to trace, but the phase sequence of their half-cycles is consistent with that of the profile horizon and with those of the detail in Figure 4. East of BSC along transect III, A and B fade by 184 km at about 90 m depth as accumulation increases

(Fig. 6). North of BSC along transect II, B fades at about 82 m depth near core site 4 (Fig. 7, bottom).

Horizon continuity is interrupted where accumulation rates vary and by artificial fading that results from trace stacking along the limbs of steeper folds. For example in Figure 3, near 100 km, the 2.7 m distance traveled between stacked traces and the maximum estimated dip of $\theta=0.53$ gives a round-trip change of distance to the horizon of only 5.0 cm, which is ~ 0.1 wavelength (48 cm in firn of $\epsilon=2.4$) of phase shift over our 32-trace stack at 400 MHz. The increased shift at higher frequencies affects the higher half of

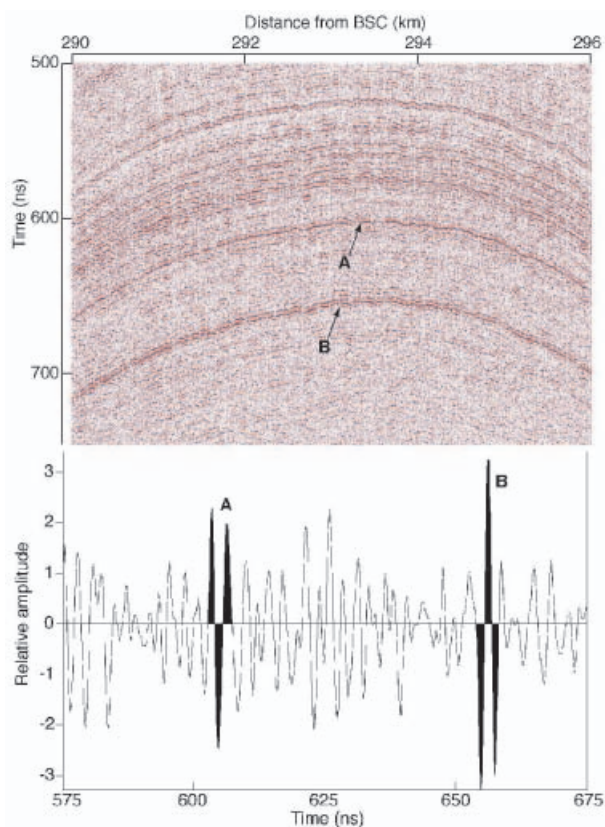


Fig. 5. Horizons A and B at 290–296 km along transect IV from BSC (top). They fade by another 40 km south. The trace (bottom) shows the major cycles of horizons A and B at 292.96 km. These phase structures are consistent with those shown in Figure 4.

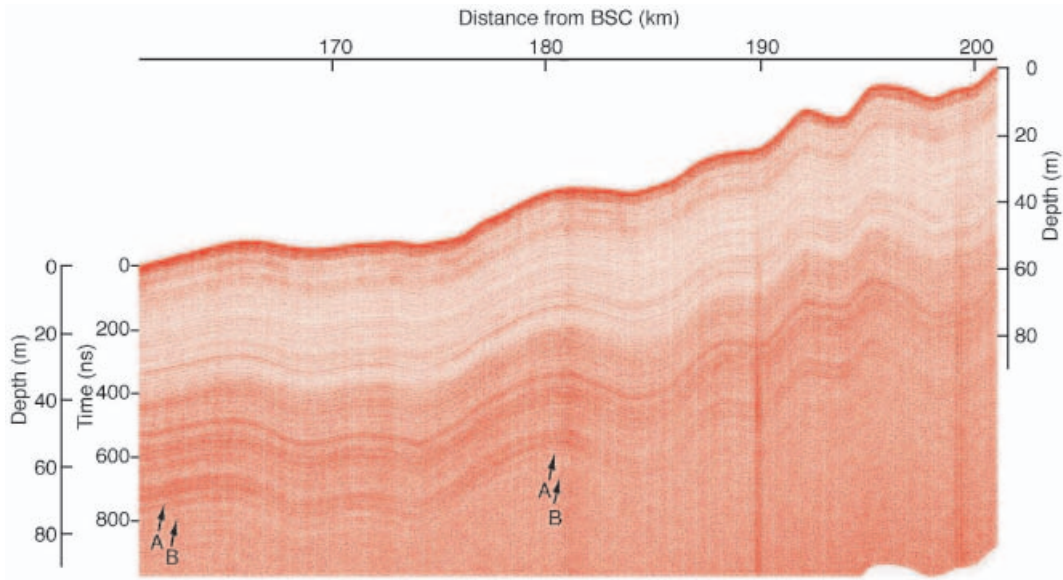


Fig. 6. Fading of horizons A and B by a depth of about 80 m along transect III. The amplitudes strengthen with depth into the firn and then begin to fade below about 75 m.

the pulse spectrum far more severely. The effect is stronger for the other transects because their speed was even greater; at a travel distance of 15 m the shift across the stack would be >0.5 wavelengths.

HORIZON AMPLITUDES AND MODELING

Although compaction with burial should decrease density contrasts, the horizons maintain their amplitude with depth well into the firn (Figs 6 and 7). In general, higher

accumulation areas (e.g. Fig. 7, top) show weaker reflections than do areas of lower accumulation (e.g. Fig. 7, bottom). The general reflectivity range is about -37 to -50 dB (Fig. 8).

We propose that the 1–2 mm thick ice layers that frequently occur in our cores, even at spacings <1 cm (Fig. 9), might explain these observations. We support this idea by modeling the pulse responses to such layers to show that constructive interference between their responses as they get closer together will maintain reflection amplitude with depth. The model of our pulse shape is shown as

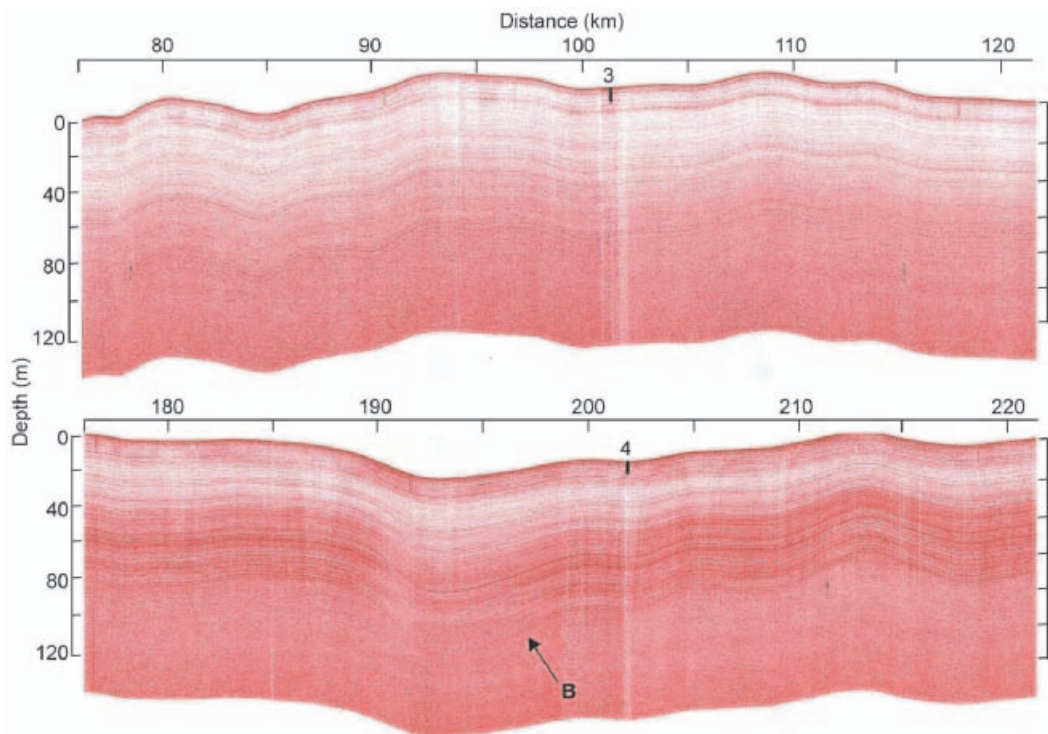


Fig. 7. Profile sections near core sites 3 and 4 (as noted) along transect II. The profile has been Hilbert transformed to represent the amplitude of wavelet envelopes. The lower profile shows the fading and loss of horizon B. Distance is measured from core site 2.

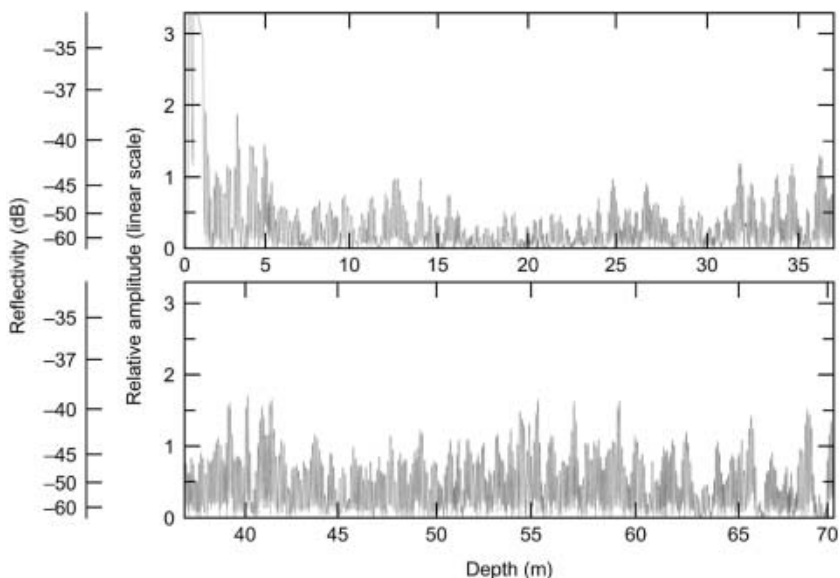


Fig. 8. Single trace amplitude also calibrated in reflectivity values relative to a perfect reflector. The traces have been rectified to allow the decibel scale for the reflectivity.

the reflection from the top of a very thick ice layer (Fig. 10, top) and its inverse, the reflection from the bottom. The reflection from a very thin ice layer in this figure is seen to be very similar in form and with a reflectivity value consistent with the range shown in Figure 8. In Figure 10 (bottom) we then show that the reflectivity for a cluster at depth is consistent with the values in Figure 8. The reversal of phase, such as between the events which compose horizon A (Fig. 4) or between A and B in Figure 5, can be explained by the occurrence of a hoar layer, which frequently occurs beneath thin ice layers because it is the source of vapor that creates the ice layer (Gow, 1968). Therefore, our thin-layer hypothesis and observed continuity scale are also consistent with interpretations of satellite radiometric data for widespread hoar events (Shuman and others, 1997).

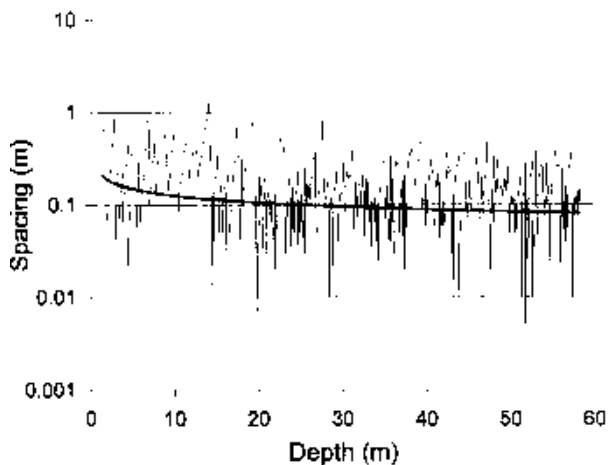


Fig. 9. The spacings between the 387 ice layers in the site 4 core (data courtesy of D. Meese and A. Gow, US Army Cold Regions Research and Engineering Laboratory) as a function of depth. Many spacings are a few cm; the heavy line shows the trend. Spacings at other sites are very similar.

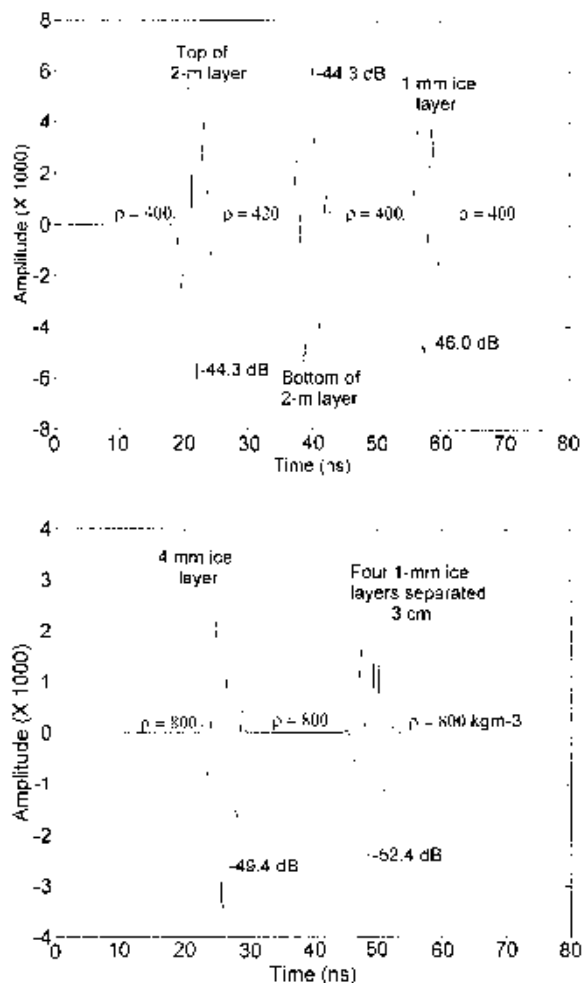


Fig. 10. A model of our pulse and its inverse are the first two reflections from a thick layer, followed by the response to a 1 mm layer of ice, all situated in shallow firm with a density of 400 kg m^{-3} (top). Both the marginal density contrast and the extreme thinness still produce detectable reflections. The responses from one and then four thin layers of ice deep within firm are at the bottom. These four layers are close enough to appear as one thicker layer and so increase the reflection amplitude.

CONCLUSIONS

The distance scale of the horizon continuity implies that the same horizons may exist extensively throughout Antarctica. Improved imaging will require either a higher trace acquisition rate or a slower towing speed, especially in areas of stronger relief, to overcome artificial fading and improve depth performance. Depth can certainly be improved by using higher-performance synthetic pulse radar (Kanagaratnam and others, 2001). It would be difficult to obtain greater resolution with higher-frequency, short-pulse radar because the fading problem would be more severe. Our benchmark horizons will allow spatial fluctuations of accumulation rates to be accurately mapped. Our argument for thin-density layers as a cause of reflections implies that the profiles may show a record of past widespread hoar and/or thin-ice layer formation events.

ACKNOWLEDGEMENTS

This work was supported by the US National Science Foundation, grants 9814589 and 088035. We thank S. Kaspari and D. Dixon of the University of Maine for their work in core dating.

REFERENCES

- Arcone, S. A. 2002. Radar profiling at 1500 ns in firn. In Koppenjan, S. and H. Lee, eds. *Ninth International Conference on Ground-Penetrating Radar, April 2002, Santa Barbara, CA. SPIE Vol. 4758*. Bellingham, WA, International Society for Optical Engineering, 433–437.
- Benson, C. S. 1971. Stratigraphic studies in the snow at Byrd Station, Antarctica, compared with similar studies in Greenland. In Crary, A. P., ed. *Antarctic snow and ice studies II*. Washington, DC, American Geophysical Union, 333–353. (Antarctic Research Series 16.)
- Black, H. P. and W. Budd. 1964. Accumulation in the region of Wilkes, Wilkes Land, Antarctica. *J. Glaciol.*, **5**(37), 3–15.
- Cumming, W. A. 1952. The dielectric properties of ice and snow at 3.2 centimeters. *J. Appl. Phys.*, **23**(7), 768–773.
- Eisen, O., F. Wilhelms, U. Nixdorf and H. Miller. 2003. Revealing the nature of radar reflections in ice: DEP-based FDTD forward modeling. *Geophys. Res. Lett.*, **30**(5), 1218–1221.
- Fujita, S. and 6 others. 1999. Nature of radio-echo layering in the Antarctic ice sheet detected by a two-frequency experiment. *J. Geophys. Res.*, **104**(B6), 13,013–13,024.
- Gow, A. J. 1968. Deep core studies of the accumulation and densification of snow at Byrd Station and Little America V, Antarctica. *CRREL Res. Rep.* 197.
- Hamilton, G. S. and V. B. Spikes. 2004. Evaluating a satellite altimeter-derived digital elevation model of Antarctica using precision kinematic GPS profiling. *Global Planet. Change*, **42**(1–4), 17–30.
- Kanagaratnam, P., S. P. Gogineni, N. Gundestrup and L. Larsen. 2001. High-resolution radar mapping of internal layers at the North Greenland Ice Core Project. *J. Geophys. Res.*, **106**(D24), 33,799–33,811.
- Kreutz, K. J., P. A. Mayewski, L. D. Meeker, M. S. Twickler and S. I. Whitlow. 2000. The effect of spatial and temporal accumulation rate variability in West Antarctica on soluble ion deposition. *Geophys. Res. Lett.*, **27**(16), 2517–2520.
- Mayewski, P. A. 2003. Antarctic oversnow traverse-based Southern Hemisphere climate reconstruction. *Transactions, American Geophysical Union*, **84**(22), 205, 210.
- Richardson, C., E. Aarholt, S.-E. Hamran, P. Holmlund and E. Isaksson. 1997. Spatial distribution of snow in western Dronning Maud Land, East Antarctica, mapped by a ground-based snow radar. *J. Geophys. Res.*, **102**(B9), 20,343–20,353.
- Shuman, C. A. and 8 others. 1997. Detection and monitoring of annual indicators and temperature trends at GISP2 using passive-microwave remote-sensing data. *J. Geophys. Res.*, **102**(C12), 26,877–26,886.
- Spikes, V. B. 2003. A mass balance study of the West Antarctic Ice Sheet. (Ph.D. thesis, University of Maine.)
- Van der Veen, C. J., E. Mosley-Thompson, A. Gow and B. G. Mark. 1999. Accumulation at South Pole: comparison of two 900-year records. *J. Geophys. Res.*, **104**(D24), 31,067–31,076.